

# Estimation of aerosol radiative effects on the terrestrial gross primary productivity in China

Zhaoyang ZHANG<sup>1</sup>, Muyuan Gao<sup>1</sup>, Qiaozhen Liu<sup>1</sup>, Yunhui Tan<sup>1</sup>, Enguang Li<sup>1</sup>, and Quan Wang<sup>2</sup>

<sup>1</sup>Zhejiang Normal University

<sup>2</sup>Faculty of Agriculture, Shizuoka University

November 23, 2022

## Abstract

China experienced heavy aerosol pollution in recent years. The aerosol pollution might change surface solar radiation and impact the land carbon cycle in China. Therefore, we combined the MODIS Atmosphere and Land products with process-based model to evaluate the sensitivity of GPP to AOD in different spectral bands under all-sky and cloudless conditions and the effects of current aerosol loadings on GPP at site level. Our results indicated that the radiative effects of aerosols on GPP varied with the vegetation type, which is consistent with other studies. We also found that the radiative effects of aerosols on GPP varied with the spectral bands. Cloud restrains the effects of aerosols on growth of plants. Current aerosol loadings fertilized the growth in two forest growth and slightly impede the growth of grass. The results in this paper could be help to fully understand the influences of aerosol on land carbon cycle.

1 **Estimation of aerosol radiative effects on**  
2 **the terrestrial gross primary productivity in**  
3 **China**

4 Zhaoyang Zhang<sup>a\*</sup>, Muyuan Gao<sup>a</sup>, Qiaozhen Liu<sup>a</sup>, Yunhui Tan<sup>a</sup>, Enguang Li<sup>a</sup>,  
5 Quan Wang<sup>b\*</sup>

6 a. College of Geography and Environmental Sciences, Zhejiang Normal  
7 University, Zhejiang Province, China

8 b. Faculty of Agriculture, Shizuoka University, Shizuoka, Japan

9

10 \*Corresponding author: Zhaoyang Zhang (zhzhyang@outlook.com), Quan Wang  
11 (wang.quan@shizuoka.ac.jp)

12

13 **Key Points:**

14 ● MODIS Atmosphere and Land products combined with the process-based model  
15 were used to accurately evaluate the aerosol effects to GPP.

16 ● The aerosol radiative effects on GPP not only varied with vegetation type but also  
17 varied with spectral regions.

18 ● Cloud restrains the effects of aerosols on growth of plants.

19

20 **Abstract**

21 China experienced heavy aerosol pollution in recent years. The aerosol pollution  
22 might change surface solar radiation and impact the land carbon cycle in China.  
23 Therefore, we combined the MODIS Atmosphere and Land products with  
24 process-based model to evaluate the sensitivity of GPP to AOD in different spectral  
25 bands under all-sky and cloudless conditions and the effects of current aerosol  
26 loadings on GPP at site level. Our results indicated that the radiative effects of  
27 aerosols on GPP varied with the vegetation type, which is consistent with other  
28 studies. We also found that the radiative effects of aerosols on GPP varied with the  
29 spectral bands. Cloud restrains the effects of aerosols on growth of plants. Current  
30 aerosol loadings fertilized the growth in two forest growth and slightly impede the  
31 growth of grass. The results in this paper could be help to fully understand the  
32 influences of aerosol on land carbon cycle.

33 **Plain Language Summary**

34 Due to the heavy aerosol pollution in China, understanding and quantifying the  
35 aerosol direct effect on plants GPP is very important in this region. To achieve this  
36 goal, MODIS Land and Atmosphere products combined with the process-based model  
37 were used. We firstly found the aerosol radiative effects on GPP not only varied with  
38 the vegetation types but also varied with the spectral regions, such as PAR and NIR.  
39 We also found that the cloud will weak the aerosol effects on GPP. The result cloud  
40 help for understanding the aerosol effects on land carbon uptake.

41

## 42 1. Introduction

43 Atmospheric aerosols contain varieties of shapes, compositions, sizes and optical  
44 properties [Hinds, 1999]. Until now, aerosol still is one of the largest uncertainties in  
45 climate studies [Field et al., 2014]. Aerosols can affect the climate changes through  
46 direct [Yu, 2004] and indirect effects [Huang et al., 2006; Zamora et al., 2017]. The  
47 direct effect is that aerosols can affect the atmospheric radiative balance through  
48 absorbing and scattering the solar radiation [Chou et al., 2006; Qian et al., 2007].  
49 Solar radiation is an essential factor for plants photosynthesis. The disturbance of  
50 solar radiation can affect plant physiological processes in two ways. First, the  
51 increasing aerosol loadings can reduce total solar radiation [Eck et al., 2013]. Second,  
52 the increasing aerosol loadings could also increase the diffuse radiation [Ceamanos et  
53 al., 2014]. Increased fraction of diffuse radiation could enhance photosynthesis to  
54 some extent [Yamaguchi and Izuta, 2017]. This was called as the diffuse radiation  
55 fertilization effect [Mercado et al., 2009].

56 Previous studies of aerosol effects on plant productivity have been conducted in  
57 many regions [Cohan et al., 2002; Ezhova et al., 2018; O'Sullivan et al., 2016; Rap et  
58 al., 2018; X. Yue and Unger, 2017]. Cohan et al. [2002] found that soybean net  
59 primary productivity (NPP) peaks under moderately thick aerosol loadings using  
60 multilayer canopy model. Niyogi et al. [2004] indicated that CO<sub>2</sub> sink increased with  
61 aerosol loadings for forest and crop land, and decreased for grassland through  
62 analyzing multi-site observations. Misson et al. [2005] showed that the increase in  
63 diffuse radiation due to aerosol can increase by 8% of CO<sub>2</sub> net uptake. Cirino et al.  
64 [2014] found that the aerosol effect accounted an approximate 20% increase in net  
65 ecosystem exchange (NEE) in Amazon. Strada et al. [2015] found that high aerosol  
66 optical depth (AOD) enhanced plant productivity by 13% in deciduous forests and  
67 had no significant effects on cropland and grassland using the satellite and surface  
68 measurements. Ezhova et al. [2018] also observed larger increase in GPP for  
69 coniferous and mixed forest. Xu Yue and Unger [2018] also found that aerosol  
70 increased GPP by  $0.05 \pm 0.30 \text{ Pg C yr}^{-1}$ .

71 China suffered heavy polluted conditions in recent years [Zhang *et al.*, 2015;  
72 Zhang *et al.*, 2019b]. The comprehensive understanding of aerosol climatology and  
73 their effects over China is very import for evaluating the global role of aerosol in  
74 environmental, climatic and terrestrial problems [Liu *et al.*, 2009; Tang *et al.*, 2014; X  
75 X Tie and Cao, 2009; Wu *et al.*, 2014]. Most of the research focused on investigating  
76 the aerosol effect on environmental and climatic problems. Only few studies  
77 investigated the effects on ecosystem in China [X Tie *et al.*, 2016]. Chameides *et al.*  
78 [1999] estimated the influence of aerosol pollution on crop yields by using coupled  
79 regional climate and air quality model. X Tie *et al.* [2016] investigated the effect of  
80 regional haze pollution on rice and wheat over China using satellite measurements  
81 and empirical model. X. Yue and Unger [2017] also access the radiative effects of  
82 aerosol pollution using combined vegetation and radiation model.

83 However, most of these studies used the aerosol from reanalysis data or simulated  
84 by model. Although they can reflect the general spatial and temporal variations of  
85 aerosols, the AOD was largely underestimated [Che *et al.*, 2019]. What is more, these  
86 studies are mainly investigate the aerosol radiative effects on plants growth at  
87 300-700 nm or 300-4000nm wavelength. Therefore, there are still large uncertainties  
88 in evaluating the influence of aerosols on land carbon uptake and the radiative effects  
89 at different spectral wavelengths in GPP is still unclear.

90 The objective in this study is to evaluate the aerosol direct effects on terrestrial  
91 gross primary productivity at site level over China, especially for different spectral  
92 wavelengths. We used Santa Barbara DISORT Atmospheric Radiative Transfer  
93 (SBDART) model and Breathing Earth System Simulator (BESS) to access the  
94 current aerosol pollution direct effects on GPP at 10 FLUXNET sites in China. Firstly,  
95 we perform sensitivity experiments to investigate the sensitivity of GPP to AOD  
96 under all-sky and cloudless conditions for each site. Then, we simulate the GPP with  
97 and without aerosol. In addition to photosynthetically active radiation (PAR), we also  
98 consider the effect of near-infrared radiation (NIR). Section 2 describes the satellite  
99 Atmosphere and Land products, radiative transfer model, and process-based model  
100 used in this paper. Section 3 shows the results of sensitivity experiments. The effects

101 of PAR and NIR induced by aerosol are shown in Section 4. Section 5 summarizes  
102 and discusses the main results.

## 103 2. Data and methods

### 104 2.1 FLUXNET data

105 FLUXNET was established to monitor the temperature, humidity, wind speed,  
106 rainfall, and atmospheric carbon dioxide using the ground-based instruments and the  
107 data from FLUXNET can be used as a reference to validate the satellite and model  
108 data. We used 10 FLUXNET stations to examine the GPP products from BESS model.  
109 Table 1 shows the specific information of these FLUXNET sites. Here, the  
110 GPP\_NT\_VUT\_REF in FLUXNET2015 dataset was used.

111 Table 1. The locations and surface type of FLUXNET in China.

Station name	Surface type	Latitude	Longitude
CN-Cha	MF	42.4025	128.0958
CN-Cng	GRA	44.5934	123.5092
CN-Dan	GRA	30.4978	91.0664
CN-Din	EBF	23.1733	112.5361
CN-Du2	GRA	42.0467	116.2836
CN-Du3	GRA	42.0551	116.2809
CN-Ha2	WET	37.6086	101.3269
CN-HaM	GRA	37.37	101.18
CN-Qia	ENF	26.7414	115.0581
CN-Sw2	GRA	41.7902	111.8971

### 112 2.2 MODIS products

113 In this paper, MODIS data were used to calculate the PAR (300-700 nm) and NIR  
114 (700-4000 nm). We used MODIS Atmosphere and Land products, including solar  
115 zenith angle (MOD07), cloud optical thickness (MOD06), white-sky albedo and  
116 black-sky albedo for visible and near infrared albedo (MCD43C3), aerosol optical  
117 depth (MCD19A2), total ozone burden (MOD07), and total column precipitable water

118 vapor (MOD07). The station values were extracted from the nearest pixels around the  
119 FLUXNET station in the MODIS products. Because the high accuracy of Multi-Angle  
120 Implementation of Atmospheric Correction (MAIAC) AOD [*Martins et al.*, 2017;  
121 *Zhang et al.*, 2019a], the data were selected to accurately simulate the radiative effects  
122 induced by the aerosols in this paper.

### 123 2.3 SBDART model

124 Santa Barbara DISORT Atmospheric Radiative Transfer (SBDART) model was  
125 developed by Institute for Computational Earth System Science, University of  
126 California in 1998. The model was designed for processing and analyzing radiative  
127 transfer problems of satellite remote sensing and atmospheric energy balance. The  
128 model can be used for calculating the radiation reached at the surface under both  
129 all-sky and cloudless days [*Ricchiazzi et al.*, 1998]. This model considers all the  
130 important absorption and scattering processes which affects UV, visible and infrared  
131 radiation. SBDART can calculate the radiance reached at the surface from 0.2 $\mu$ m to  
132 100 $\mu$ m with an interval of 5nm-200nm. SBDART has been used for many researches  
133 and good performance was shown [*Frouin and Murakami*, 2007; *Nagorski et al.*, 2019;  
134 *Wong et al.*, 2008]. The aerosol type was set as rural aerosol. In this study, SBDART  
135 model was used to simulate the radiance at ground surface.

### 136 2.4 BESS model

137 In this paper, process-based model was used because it is able to provide response  
138 to environment changes, such as global warming and elevated carbon dioxide. The  
139 Breathing Earth System Simulator (BESS) is a simplified process-based model, which  
140 can simulate the canopy carbon and water fluxes, and quantified the PAR and NIR  
141 effects for sunlit and shade leaves. The model was developed by *Ryu et al.* [2018] and  
142 integrated with remote sensing data. The model can take full advantages of MODIS  
143 products [*Jiang and Ryu*, 2016]. *Ryu et al.* [2011] and *Jiang and Ryu* [2016] evaluated  
144 the performance of BESS model using FLUXNET observations and the results  
145 indicated that the model simulations were comparable with FLUXNET observations  
146 and MPI-BGC products. The BESS model code can be freely obtained from the  
147 environmental ecology lab in Seoul national university

148 ([http://environment.snu.ac.kr/bess\\_flux/](http://environment.snu.ac.kr/bess_flux/)). Some input data for FLUXNET sites were  
149 also included in the package. To investigate the aerosol radiative effects on GPP, we  
150 did four experiments (Table 2).

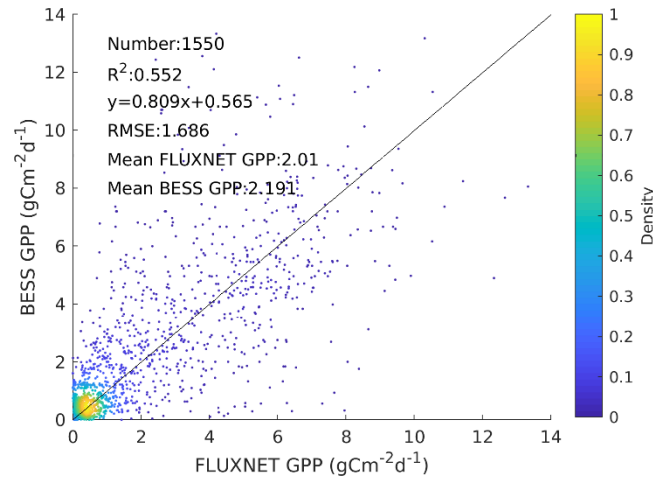
151 Table 2. Experiments design for this study.

Experiments	Description
E1	GPP simulated without aerosol for PAR calculation and without aerosol for NIR calculation
E2	GPP simulated with aerosol for PAR calculation and without aerosol for NIR calculation
E3	GPP simulated without aerosol for PAR calculation and with aerosol for NIR calculation
E4	GPP simulated with aerosol for PAR calculation and with aerosol for NIR calculation

152

### 153 3. BESS simulation and FLUXNET GPP comparison

154 Firstly, we evaluate the accuracy of GPP simulated by BESS model. Due to the  
155 comprehensive validation studies of BESS simulation [*Jiang and Ryu, 2016; Ryu et*  
156 *al., 2011*], here we only validate the general performance of BESS simulation in  
157 China. Figure 1 shows the scatter plots of FLUXNET GPP observations against BESS  
158 GPP simulations. The black line is the one-to-one line. These scatters are distributed  
159 around the line. The sample size is about 1550 with  $R^2$  of 0.552. Most of GPP values  
160 range from 0 to 1. This is might due to the low GPP in GRA FLUXNET sites. The  
161 RMSE is about 1.686. The GPP simulations from BESS are a little larger than  
162 FLUXNET GPP observations.



163

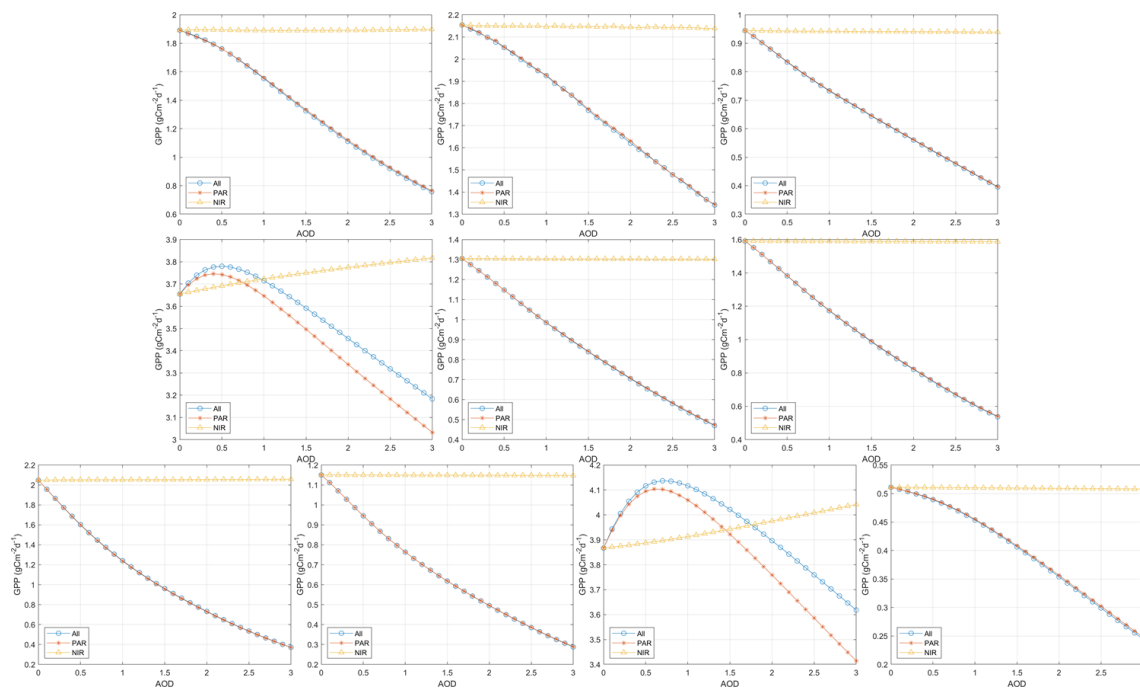
164 Figure 1. Scatter plots of BESS GPP simulations and FLUXNET measurements  
 165 (black line represents the 1:1 line).

166 **4. Sensitivity of GPP to AOD at FLUXNET sites**

167 In order to evaluate the sensitivity of GPP to AOD, AOD from 0 to 3 at an interval  
 168 of 0.1 was set for all days during 2002 to 2015. The PAR and NIR was calculated  
 169 using SBDART with different AOD bins. Then, the GPP can be obtained through  
 170 BESS model with a series of PAR and NIR. For each AOD bin, we did four  
 171 experiments (Table 2). Figure 2 shows the variations of GPP with the increasing AOD.  
 172 Yellow line means that only aerosol radiative effects in NIR was considered (E3-E1).  
 173 Red line shows that only aerosol radiative effects in PAR was calculated for accessing  
 174 the aerosol effects on GPP (E2-E1). Blue line represents that aerosol radiative effects  
 175 in both NIR and PAR were included (E4-E1). The aerosol effects in NIR have little  
 176 impacts on GPP over grassland and the GPP decreases with the increasing AOD in  
 177 this kind of surface type. For forest sites, the aerosol effects in NIR is able to enhance  
 178 the GPP and the fertilization of the aerosol effects in NIR increases with the aerosol  
 179 loadings. Fertilization of aerosol effects in PAR can be found when the AOD is lower  
 180 than 0.4/0.6 for two forest FLUXNET station. If the  $AOD > 0.4/0.6$ , the fertilization of  
 181 aerosol effects in PAR will decrease with AOD. Considering the aerosol effects in  
 182 both PAR and NIR, the maximum GPP can be found when the AOD is 0.5 for CN-Din  
 183 and 0.7 for CN-Qia. The aerosol could hinder the growth of forest when AOD is

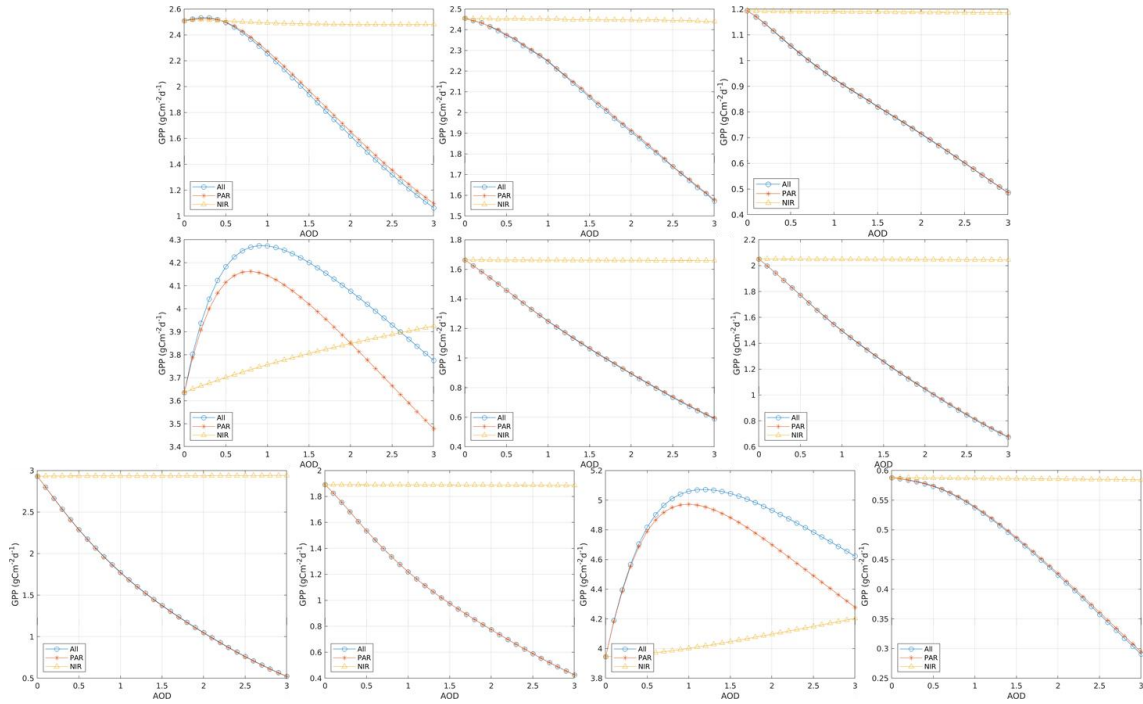
184 greater than 1.4 for CN-Din and 2.1 for CN-Qia.

185 To evaluate the effects of cloud on the interaction of aerosol and plants, we also  
186 examine the sensitivity of GPP to AOD over cloudless conditions. In this situation, we  
187 assumed that there is no cloud during the whole study period. Figure 3 illustrates the  
188 sensitivity of GPP to AOD under cloudless condition. Compared with cloudy  
189 conditions, higher GPP is shown for all FLUXNET stations. For mixed forest site, the  
190 GPP increases with the aerosol loadings when the AOD is lower than 0.4 and then the  
191 GPP decreases with the AOD. This trend cannot be simulated in all-sky conditions.  
192 For grass stations, little differences of GPP decreasing trends between all-sky and  
193 cloudless conditions are found. However, the variations of GPP are larger under  
194 cloudless conditions than that under all-sky conditions. When we only consider the  
195 aerosol effects in PAR, the maximum GPP can be found when AOD is 0.8 for CN-Din  
196 and 1 for CN-Qia. The fertilization effects of aerosols in NIR are shown in both clear  
197 days and hazy days. The GPP rises from  $\sim 3.6$  to  $\sim 3.9$   $\text{gCm}^{-2}\text{d}^{-1}$  for CN-Din and from  
198  $\sim 3.9$  to  $\sim 4.2$   $\text{gCm}^{-2}\text{d}^{-1}$  for CN- Qia. Considering aerosol effects in both PAR and NIR,  
199 maximum GPP can be found when AOD is 1 and 1.2 for EBF and ENF site. When the  
200 AOD is higher than 1-1.2, the GPP start falling. However, the fertilization effects still  
201 exist when the AOD reach to 3.



202

203 Figure 2. The sensitivity of GPP to AOD at ten FLUXNET sites (yellow line, red line,  
 204 and blue line represent the effects of NIR, PAR, and all bands).



205

206

Figure 3. Same as Figure 2, but for cloudless condition.

## 207 5. The effects of aerosol pollution on GPP

208 To evaluate the radiative effects of current aerosol pollution on GPP, we used the  
 209 MAIAC AOD, which is the most accurate aerosol products. Table 3 shows the effect  
 210 of current aerosol loadings on GPP at FLUXNET sites in China. The result indicates  
 211 that the effects of aerosol in PAR band reduce the growth of grass and mixed forests  
 212 and enhance the growth of both EBF and ENF. The effects of aerosols on GPP in NIR  
 213 is positive in EBF and ENF. Little impacts of aerosols on GPP in NIR are shown in  
 214 MF, GRA, and WET FLUXNET sites. For effects of PAR, largest variation is shown  
 215 in CN-Qia. For effects of NIR, most significant variation is shown in CN-Din. In all,  
 216 the effects of current aerosol loadings on GPP is negative in MF, GRA, and WET, and  
 217 positive in EBF and ENF.

218 Table 3. The multi-year effects of current aerosol pollutions on GPP at ten FLUXNET

219

sites.

Station name	PAR	NIR	PAR and NIR
--------------	-----	-----	-------------

CN-Cha	-0.0915	0.0019	-0.0891
CN-Cng	-0.0788	-0.0020	-0.0788
CN-Dan	-0.0073	-0.0001	-0.0074
CN-Din	0.0643	<b>0.0397</b>	0.1042
CN-Du2	-0.0800	0.0006	-0.0790
CN-Du3	-0.0990	-0.0003	-0.0993
CN-Ha2	-0.1428	0.0016	-0.1412
CN-HaM	-0.0580	-0.0001	-0.0581
CN-Qia	<b>0.1688</b>	0.0186	<b>0.1867</b>
CN-Sw2	-0.0112	-0.0001	-0.0113

220

221 Table 4. The seasonal effects of current aerosol pollution on GPP at ten FLUXNET  
222 sites.

## 223 6. Discussion and conclusions

224 In this paper, we used the MODIS Atmosphere and Land products combined with  
225 the process-based model to test the sensitivity of GPP on AOD in all-sky and  
226 cloudless conditions and accurately evaluate the current aerosol loadings on terrestrial  
227 carbon fluxes in China. We found that the aerosol radiative effects on GPP not only  
228 varied with vegetation type but also varied with the spectral regions. The difference of  
229 aerosol effects in vegetation types are widely acknowledged [Ezhova *et al.*, 2018;  
230 Niyogi *et al.*, 2004]. However, the aerosol radiative effects on GPP in different  
231 spectral regions were seldom reported in our knowledge. The differences in spectral  
232 regions are because they have different features in atmospheric and canopy radiative  
233 transfer. In atmosphere, the magnitude of NIR influenced by aerosols is smaller than  
234 that of PAR [Hatzianastassiou *et al.*, 2007]. In addition, the photons are scattered  
235 more in the NIR region than PAR within the canopy [Ryu *et al.*, 2011]. These are the  
236 two mainly reasons for the difference of aerosol effects on GPP in PAR and NIR.

237 The estimation in this paper is highly dependent on the capacity of the BESS

238 model. Therefore, we assessed the performance of BESS GPP simulations against  
239 FLUXNET observations in China. The GPP simulated by FLUXNET can agree with  
240 the ground-based measurements well ( $R^2 > 0.55$ ). The satellite AOD is also one of the  
241 uncertainties for simulating the radiative effects of aerosols. Previous study has  
242 demonstrated that the MAIAC aerosol products are highly consistent with the  
243 ground-based measurements in China ( $R > 0.92$ ) [Zhang *et al.*, 2019a]. The accuracy of  
244 MAIAC AOD is higher than model simulations [Sun *et al.*, 2019]. Therefore, we  
245 consider our results have high accuracy in simulating the aerosol radiative effects.  
246 Here, we only considered the aerosol radiative effects and ignored the environment  
247 effects of aerosols, such as temperature, vapor pressure deficit (VPD) and  
248 precipitation. Huang *et al.* [2006] examined the impacts of aerosols on surface  
249 temperature and found that the diurnal temperature range decreases by  $-0.7^\circ\text{C}$  over the  
250 industrialized regions in China. Lee *et al.* [2014] estimated that the precipitation  
251 reduction is about 40% due to the effects of absorbing aerosols. However, these  
252 papers also showed that the confidence of the result is limited by the uncertainties in  
253 modelling cloud physics. In addition, the ground-based measurements of  
254 aerosol-precipitation and aerosol-temperature interactions are still very limited and  
255 hardly to find a consistent conclusion. Therefore, only aerosol radiative effects were  
256 considered.

257 Although there are still some uncertainties, we firstly showed that aerosol  
258 radiative effects on GPP varied with vegetation type and spectral band. For NIR  
259 (700-4000 nm), little impacts of aerosols were shown over grass and wet land, while  
260 the forest GPP monotonously increased with the aerosol loadings when the AOD is  
261 lower than 3. For PAR (300-700), The GPP in grass land decreased with the AOD and  
262 the forest GPP firstly increases with the AOD and then decreased. The clouds play an  
263 important role in the aerosols-plants interaction and they restrain the effects of  
264 aerosols on growth of plants. The conclusion in this study can be used for fully  
265 understanding the effects of aerosol on land carbon uptake.

266 **Acknowledgements**

267 The authors would like to thank the team of BESS model  
268 ([http://environment.snu.ac.kr/bess\\_flux/](http://environment.snu.ac.kr/bess_flux/)) for their hard work. We appreciate a large  
269 work of MODAPS team on MAIAC integration. We would like to thank the team of  
270 MODIS (<https://ladsweb.modaps.eosdis.nasa.gov/search/>) and FLUXNET  
271 (<https://fluxnet.fluxdata.org/data/fluxnet2015-dataset/>) for their great work. This study  
272 was supported by the Zhejiang Provincial Natural Science Foundation of China  
273 (Grant No. LQ18D010004), National Science Foundation of China (Grant No.  
274 41801258).

275

276 **References:**

277 Ceamanos, X., D. Carrer, and J. L. Roujean (2014), Improved retrieval of direct and diffuse downwelling  
278 surface shortwave flux in cloudless atmosphere using dynamic estimates of aerosol content and type:  
279 application to the LSA-SAF project, *Atmospheric Chemistry and Physics*, *14*(15), 8209-8232.

280 Chameides, W. L., et al. (1999), Case study of the effects of atmospheric aerosols and regional haze on  
281 agriculture: An opportunity to enhance crop yields in China through emission controls?, *Proceedings*  
282 *of the National Academy of Sciences*, *96*(24), 13626.

283 Che, H., et al. (2019), Large contribution of meteorological factors to inter-decadal changes in regional  
284 aerosol optical depth, *Atmos. Chem. Phys.*, *19*(16), 10497-10523.

285 Chou, M.-D., P.-H. Lin, P.-L. Ma, and H.-J. Lin (2006), Effects of aerosols on the surface solar radiation in  
286 a tropical urban area, *Journal of Geophysical Research: Atmospheres*, *111*(D15), D15207.

287 Cirino, G. G., R. A. F. Souza, D. K. Adams, and P. Artaxo (2014), The effect of atmospheric aerosol  
288 particles and clouds on net ecosystem exchange in the Amazon, *Atmos. Chem. Phys.*, *14*(13),  
289 6523-6543.

290 Cohan, D. S., J. Xu, R. Greenwald, M. H. Bergin, and W. L. Chameides (2002), Impact of atmospheric  
291 aerosol light scattering and absorption on terrestrial net primary productivity, *Global Biogeochemical*  
292 *Cycles*, *16*(4), 37-31-37-12.

293 Eck, T. F., J. Huttunen, K. E. J. Lehtinen, A. V. Lindfors, G. Myhre, A. Smirnov, S. N. Tripathi, and H. Yu  
294 (2013), Influence of observed diurnal cycles of aerosol optical depth on aerosol direct radiative effect,

295 *Atmospheric Chemistry and Physics*, 13(15), 7895-7901.

296 Ezhova, E., et al. (2018), Direct effect of aerosols on solar radiation and gross primary production in  
297 boreal and hemiboreal forests, *Atmos. Chem. Phys.*, 18(24), 17863-17881.

298 Field, C. B., V. R. Barros, K. Mach, and M. Mastrandrea (2014), Climate change 2014: impacts,  
299 adaptation, and vulnerability, *Working Group II Contribution to the IPCC 5th Assessment*  
300 *Report-Technical Summary*, 1-76.

301 Frouin, R., and H. Murakami (2007), Estimating photosynthetically available radiation at the ocean  
302 surface from ADEOS-II global imager data, *Journal of Oceanography*, 63(3), 493-503.

303 Hatzianastassiou, N., C. Matsoukas, A. Fotiadi, J. P. W. Stackhouse, P. Koepke, K. G. Pavlakis, and I.  
304 Vardavas (2007), Modelling the direct effect of aerosols in the solar near-infrared on a planetary scale,  
305 *Atmos. Chem. Phys.*, 7(12), 3211-3229.

306 Hinds, W. C. (1999), *Aerosol Technology: Properties, Behavior, and Measurement of airborne Particles*  
307 (2nd).

308 Huang, Y., R. E. Dickinson, and W. L. Chameides (2006), Impact of aerosol indirect effect on surface  
309 temperature over East Asia, *Proceedings of the National Academy of Sciences of the United States of*  
310 *America*, 103(12), 4371.

311 Jiang, C., and Y. Ryu (2016), Multi-scale evaluation of global gross primary productivity and  
312 evapotranspiration products derived from Breathing Earth System Simulator (BESS), *Remote Sensing of*  
313 *Environment*, 186, 528-547.

314 Lee, D., Y. C. Sud, L. Oreopoulos, K. M. Kim, W. K. Lau, and I. S. Kang (2014), Modeling the influences of  
315 aerosols on pre-monsoon circulation and rainfall over Southeast Asia, *Atmospheric Chemistry and*  
316 *Physics*, 14(13), 6853-6866.

317 Liu, Y., J. R. Sun, and B. Yang (2009), The effects of black carbon and sulphate aerosols in China regions  
318 on East Asia monsoons, *Tellus Series B-Chemical and Physical Meteorology*, 61(4), 642-656.

319 Martins, V. S., A. Lyapustin, L. A. S. de Carvalho, C. C. F. Barbosa, and E. M. L. M. Novo (2017),  
320 Validation of high-resolution MAIAC aerosol product over South America, *J Geophys Res-Atmos*,  
321 122(14), 7537-7559.

322 Mercado, L. M., N. Bellouin, S. Sitch, O. Boucher, C. Huntingford, M. Wild, and P. M. Cox (2009), Impact  
323 of changes in diffuse radiation on the global land carbon sink, *Nature*, 458(7241), 1014-1017.

324 Misson, L., M. Lunden, M. McKay, and A. H. Goldstein (2005), Atmospheric aerosol light scattering and

325 surface wetness influence the diurnal pattern of net ecosystem exchange in a semi-arid ponderosa  
326 pine plantation, *Agricultural and Forest Meteorology*, 129(1), 69-83.

327 Nagorski, S. A., S. D. Kaspari, E. Hood, J. B. Fellman, and S. M. Skiles (2019), Radiative Forcing by Dust  
328 and Black Carbon on the Juneau Icefield, Alaska, *Journal of Geophysical Research: Atmospheres*, 0(ja).

329 Niyogi, D., et al. (2004), Direct observations of the effects of aerosol loading on net ecosystem CO<sub>2</sub>  
330 exchanges over different landscapes, *Geophysical Research Letters*, 31(20).

331 O'Sullivan, M., A. Rap, C. L. Reddington, D. V. Spracklen, M. Gloor, and W. Buermann (2016), Small  
332 global effect on terrestrial net primary production due to increased fossil fuel aerosol emissions from  
333 East Asia since the turn of the century, *Geophysical Research Letters*, 43(15), 8060-8067.

334 Qian, Y., W. G. Wang, L. R. Leung, and D. P. Kaiser (2007), Variability of solar radiation under cloud-free  
335 skies in China: The role of aerosols, *Geophysical Research Letters*, 34(12), L12804.

336 Rap, A., et al. (2018), Enhanced global primary production by biogenic aerosol via diffuse radiation  
337 fertilization, *Nature Geoscience*, 11(9), 640-644.

338 Ricchiazzi, P., S. Yang, C. Gautier, and D. Sowle (1998), SBDART: A Research and Teaching Software Tool  
339 for Plane-Parallel Radiative Transfer in the Earth's Atmosphere, *B Am Meteorol Soc*, 79(10), 2101-2114.

340 Ryu, Y., C. Jiang, H. Kobayashi, and M. Detto (2018), MODIS-derived global land products of shortwave  
341 radiation and diffuse and total photosynthetically active radiation at 5km resolution from 2000,  
342 *Remote Sensing of Environment*, 204, 812-825.

343 Ryu, Y., et al. (2011), Integration of MODIS land and atmosphere products with a coupled-process  
344 model to estimate gross primary productivity and evapotranspiration from 1 km to global scales,  
345 *Global Biogeochemical Cycles*, 25(4).

346 Strada, S., N. Unger, and X. Yue (2015), Observed aerosol-induced radiative effect on plant productivity  
347 in the eastern United States, *Atmospheric Environment*, 122, 463-476.

348 Sun, E., X. Xu, H. Che, Z. Tang, K. Gui, L. An, C. Lu, and G. Shi (2019), Variation in MERRA-2 aerosol  
349 optical depth and absorption aerosol optical depth over China from 1980 to 2017, *Journal of*  
350 *Atmospheric and Solar-Terrestrial Physics*, 186, 8-19.

351 Tang, J., P. Wang, L. J. Mickley, X. Xia, H. Liao, X. Yue, L. Sun, and J. Xia (2014), Positive relationship  
352 between liquid cloud droplet effective radius and aerosol optical depth over Eastern China from  
353 satellite data, *Atmospheric Environment*, 84(0), 244-253.

354 Tie, X., R. J. Huang, W. Dai, J. Cao, X. Long, X. Su, S. Zhao, Q. Wang, and G. Li (2016), Effect of heavy

355 haze and aerosol pollution on rice and wheat productions in China, *Sci Rep*, 6, 29612.

356 Tie, X. X., and J. J. Cao (2009), Aerosol pollution in China: Present and future impact on environment,  
357 *Particuology*, 7(6), 426-431.

358 Wong, M. S., J. Nichol, K. H. Lee, and Z. Li (2008), Retrieval of aerosol optical thickness using MODIS  
359 500× 500m 2, a study in Hong Kong and Pearl River Delta region, paper presented at Earth  
360 Observation and Remote Sensing Applications, 2008. EORSA 2008. International Workshop on, IEEE.

361 Wu, S., et al. (2014), Association of cardiopulmonary health effects with source-appointed ambient  
362 fine particulate in Beijing, China: a combined analysis from the Healthy Volunteer Natural Relocation  
363 (HVNR) study, *Environmental science & technology*, 48(6), 3438-3448.

364 Yamaguchi, M., and T. Izuta (2017), Effects of Aerosol Particles on Plants, in *Air Pollution Impacts on*  
365 *Plants in East Asia*, edited by T. Izuta, pp. 283-293, Springer Japan, Tokyo.

366 Yu, H. (2004), Direct radiative effect of aerosols as determined from a combination of MODIS retrievals  
367 and GOCART simulations, *Journal of Geophysical Research*, 109(D3).

368 Yue, X., and N. Unger (2017), Aerosol optical depth thresholds as a tool to assess diffuse radiation  
369 fertilization of the land carbon uptake in China, *Atmos. Chem. Phys.*, 17(2), 1329-1342.

370 Yue, X., and N. Unger (2018), Fire air pollution reduces global terrestrial productivity, *Nature*  
371 *Communications*, 9(1), 5413.

372 Zamora, L. M., R. A. Kahn, S. Eckhardt, A. McComiskey, P. Sawamura, R. Moore, and A. Stohl (2017),  
373 Aerosol indirect effects on the nighttime Arctic Ocean surface from thin, predominantly liquid clouds,  
374 *Atmos. Chem. Phys.*, 17(12), 7311-7332.

375 Zhang, Z. Y., M. S. Wong, and K. H. Lee (2015), Estimation of potential source regions of PM2.5 in  
376 Beijing using backward trajectories, *Atmospheric Pollution Research*, 6(1), 173-177.

377 Zhang, Z. Y., W. L. Wu, M. Fan, J. Wei, Y. H. Tan, and Q. Wang (2019a), Evaluation of MAIAC aerosol  
378 retrievals over China, *Atmospheric Environment*, 202, 8-16.

379 Zhang, Z. Y., W. L. Wu, M. Fan, M. H. Tao, J. Wei, J. Jin, Y. H. Tan, and Q. Wang (2019b), Validation of  
380 Himawari-8 aerosol optical depth retrievals over China, *Atmospheric Environment*, 199, 32-44.

381